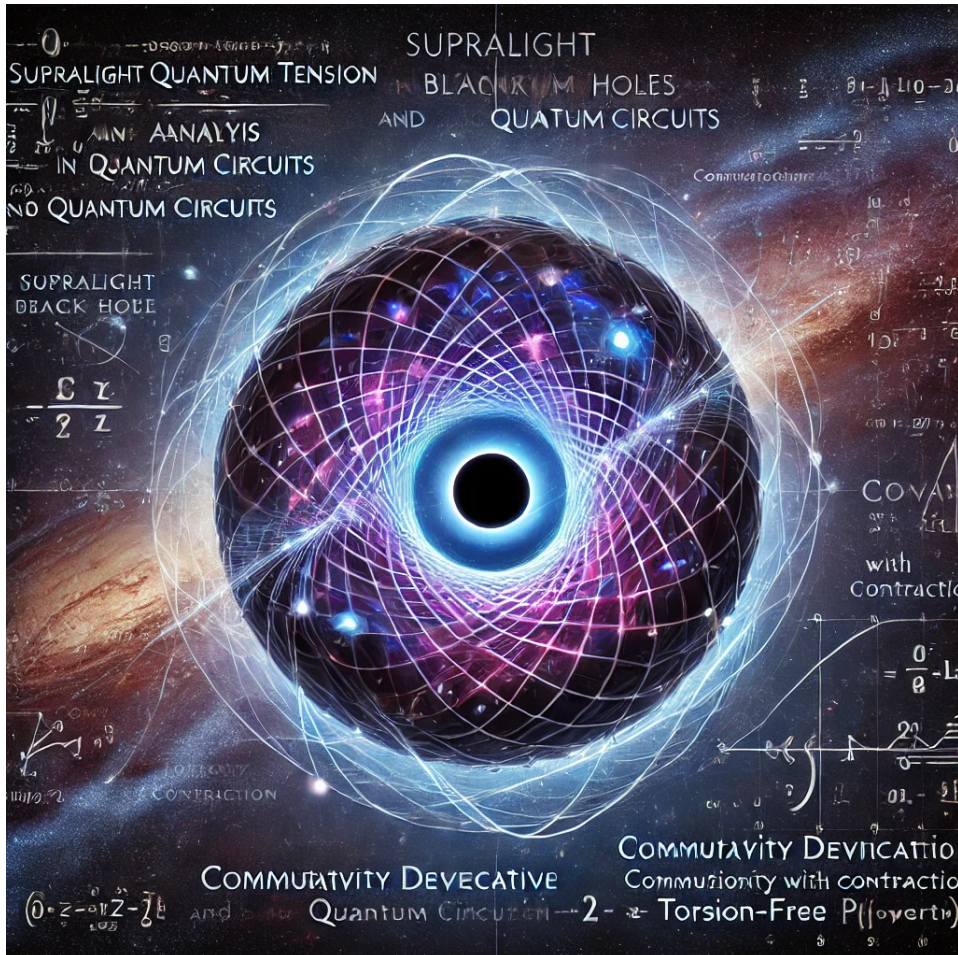


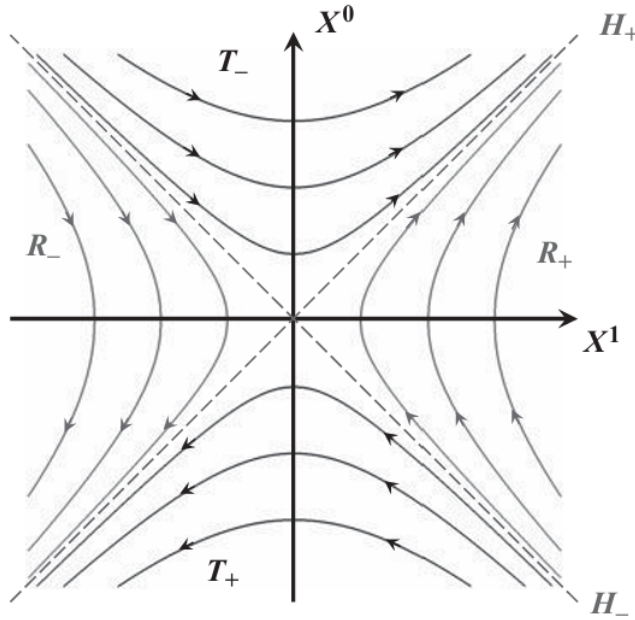
Supralight Quantum Tension: An Analysis in Black Holes and Quantum circuits



Covariant derivative: 1. Commutativity with contraction: $\nabla_\mu(A_{\alpha\ldots\beta\ldots}) = (\nabla_\mu A)_{\alpha\ldots\beta\ldots}$.
 2. For a scalar field: $\nabla_\mu \phi = \phi_{,\mu}$.
 3. Torsion free: $\nabla_\mu \nabla_\nu \phi = \nabla_\nu \nabla_\mu \phi$. 6. $\nabla_\mu \alpha_\beta = 0$.

These properties determine the covariant derivative and hence they can be used as its definition. Consider a line γ and let ξ be its tangent vector. A tensor field $A_{\alpha\ldots\beta\ldots}$ is called parallel transport along γ if $\xi^\mu \nabla_\mu A_{\alpha\ldots\beta\ldots} = 0$.

Properties-spaces:



Integral lines of the boost Killing vector in the $(X^0 - X^1)$ -plane. These lines are future directed in R^+ and are past directed in R^- . In T^\pm they are space-like. These integral lines are tangent to the horizons H^\pm and coincide there with the horizon generators.

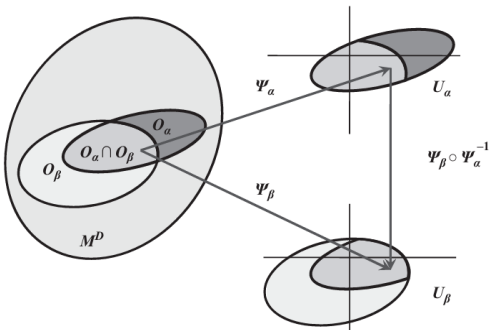
Lie & Fermi Transport

3.4.1 variables

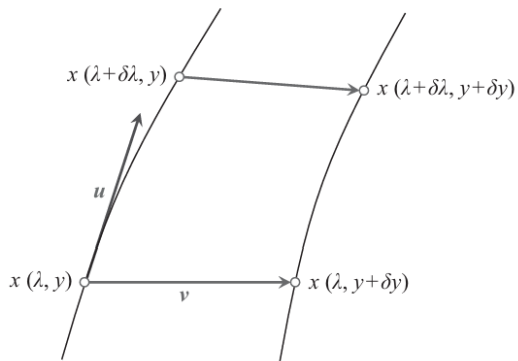
The lines $x^\mu(\lambda, y_i)$, where y_i ‘enumerates’ lines, and λ is a parameter along a line. For this congruence $u^\mu = \partial x^\mu / \partial \lambda$ is a tangent vector to a line, and $v^\mu = (\partial x^\mu / \partial y_i) \delta y_i$ is a vector connecting two lines of the congruence with the same value of λ and with the parameters y_i and $y_i + \delta y_i$, respectively.

3.3.2 Properties of the covariant derivative The covariant derivative possesses the following properties: 1. Linearity: For constants a and b one has $\nabla^\mu(aA_{\mu\nu}... + bB_{\mu\nu}...) = a\nabla^\mu A_{\mu\nu}... + b\nabla^\mu B_{\mu\nu}...$ 2. Leibnitz rule: $\nabla^\mu(A_{\mu\nu}... B_{\nu\rho}...) = \nabla^\mu A_{\mu\nu}... B_{\nu\rho}... + A_{\mu\nu}... \nabla^\mu B_{\nu\rho}...$

3. Commutativity with contraction: $\nabla^\mu(A_{\mu\nu}...\beta_{\nu\rho}...) = (\nabla^\mu A_{\mu\nu})...\beta_{\nu\rho}... + A_{\mu\nu}...\nabla^\mu\beta_{\nu\rho}...$
4. For a scalar field: $\nabla^\mu\phi = \phi,\mu$.
5. Torsion free: $\nabla^\mu\nabla^\nu\phi = \nabla^\nu\nabla^\mu\phi$.
6. $\nabla^\mu\alpha\beta = 0$. These properties unambiguously determine the covariant derivative and hence they can be used as its definition. Consider a line γ and let ξ be its tangent vector. A tensor field $A_{\alpha\mu}\beta^\mu$ is called parallel transport along γ if $\xi^\mu \nabla_\mu A_{\alpha\mu}\beta^\mu = 0$.



Vectorization process is described as a vector field generating a one-parameter group of diffeomorphisms. The Lie derivative $L\xi A\alpha... \beta...$ of a tensor field $A\alpha... \beta...$ along $\xi\mu$ is defined by the relation $L\xi A\alpha... \beta... = \lim_{\lambda \rightarrow 0} f^* -\lambda A\alpha... \beta... - A\alpha... \beta... \lambda$. The following explicit expressions are valid for the Lie derivative .
 $L\xi A\alpha... \beta... = \xi\mu \partial\mu A\alpha... \beta... - \partial\mu\xi\alpha A\mu... \beta... - \dots + \partial\beta\xi\mu A\alpha... \mu... + \dots = \xi\mu \nabla\mu A\alpha... \beta... - \nabla\mu\xi\alpha A\mu... \beta... - \dots + \nabla\beta\xi\mu A\alpha... \mu... + \dots$.



The Lie derivative obeys the following relations 1. $L\xi\xi = 0$; 2. $L\xi(\alpha A\alpha... \beta... + \beta B\alpha... \beta...) = \alpha L\xi A\alpha... \beta... + \beta L\xi B\alpha... \beta...$ 3. $L\xi(A\alpha... \beta... B\alpha... \beta...) = L\xi A\alpha... \beta... B\alpha... \beta...$ 4. $L\xi H - L\xi L\xi = L[\xi, \eta]$. . . (α and β are arbitrary constants); . . . + A\alpha... \beta... L\xi B\alpha... \beta...; Atensor field $A\alpha... \beta...$ is said to be Lie-transported along ξ if $L\xi A\alpha... \beta... = 0$.

Riemannian Geometry the vector u that can be defined for any tensor field (see later). The Lie derivative of the vector v coincides with the commutator $(Luv)\mu = [u, v]\mu$.

Tensor-vector: A tensor one can construct a new operation, called a Fermi derivative. The Fermi derivative $F\xi A\alpha... \beta...$ of a tensor field $A\alpha... \beta...$ along a vector field ξ ($\xi\mu \xi\mu = 0$) is defined as: $F\xi A\alpha... \beta... = \xi\mu \nabla\mu A\alpha... \beta... + F A\alpha... \beta... + \dots - B\sigma\beta A\alpha... \sigma... + \dots$.

Atensor field $A\alpha... \beta...$ is said to be Fermi-transported along ξ if $F\xi A\alpha... \beta... = 0$.

1. $F G\mu\nu = 0$.

For a geodesic congruence the tensor F vanishes and the Fermi derivative $F\xi$ coincides with the covariant one $\xi\mu \nabla\mu$.

3.5.1 Commutator of covariant derivative In a flat spacetime two covariant derivatives commute. Non-commutativity of the covariant derivatives implies that the spacetime is curved. Using the definition

of the covariant derivative Eq. (3.3.4), straightforward calculations give $V\beta;\mu\nu - V\beta;\nu\mu = V\alpha R\alpha\beta\mu\nu = V\alpha R\alpha\beta\mu\nu$.

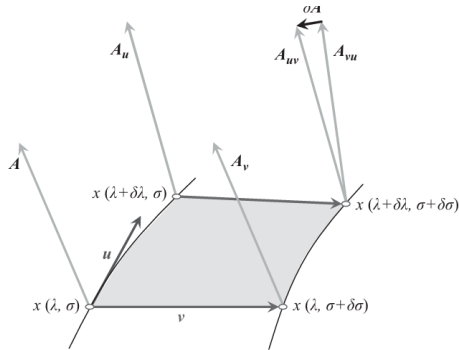
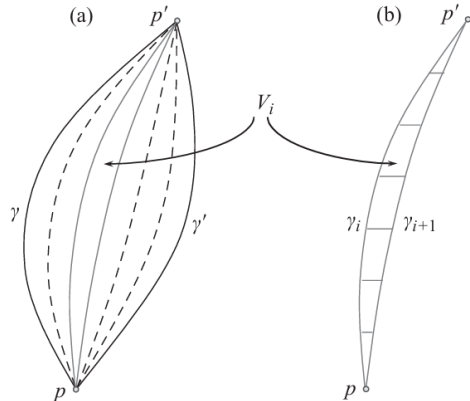


Fig. 3.10 The result of a parallel transport of a vector A depends on a path. Two vectors obtained from A by the parallel transport from an initial point p to a final point p' along ‘upper’ (p, p') and ‘lower’ (p, p') paths differ by the vector δA . $\delta I\alpha = \alpha\beta\gamma\delta\beta\gamma\delta\lambda\delta\sigma$.

Fig. 3.11 Illustration of the proof of the theorem. The left figure (a) shows a one-parameter family of curves connecting two points p and p' in a simply connected region. The right figure (b) shows a surface element between two nearby curves γ_i and γ_{i+1} .



$$\text{Eq: } g_{\mu\nu}(p)\epsilon^\mu \wedge \alpha(p)\epsilon^\nu \wedge \beta(p) = \eta \wedge \alpha \wedge \beta.$$

Operators in black-holes:

Riemannian operator For any two vectors u and v the Riemannian operator $R(u,v)$ acting on a third vector w is defined by the relation $R(u,v)w = (\nabla u \nabla v - \nabla v \nabla u - \nabla [u,v])w$.

Let us show that

1. $(R(u,v)w)\mu = M v\beta v u\alpha v\beta$.
2. The right-hand side of Eq. (3.6.29) is $u\alpha(v\beta w\mu; \beta); \alpha - v\alpha(u\beta w\mu; \beta); \alpha - (u\alpha v\beta; \alpha - v\alpha u\beta; \alpha)w\mu; \beta = u\alpha v\beta(w\mu; \beta\alpha\mu; \alpha\beta) = M\alpha\beta\gamma\alpha B$.

Geodesic relations:

$$R(u,n)u = \nabla u \nabla n - \nabla n \nabla u u = \nabla u \nabla n u = \nabla u \nabla un.$$

The geodesic equation $\nabla uu = 0$ and the relation Eq. (3.6.32) that implies that $\nabla nu = \nabla un$.

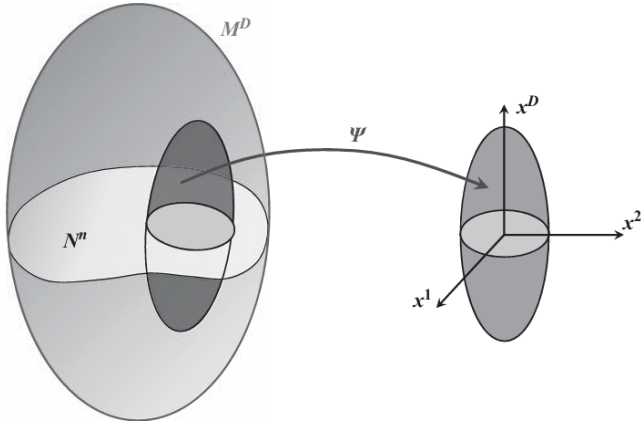


Fig. 4.5 Two foliations t and t of the phase space are shown. At the initial moment $t = 0$ the foliation surfaces coincide. The fiducial geodesic intersects the foliation surfaces t and t at a point p . u and u are unit time-like vectors at p orthogonal to and, $\Sigma_0 \Pi p$ respectively.

4.3.1 Liouville theorem on complete integrability Integrability is an important property of some dynamical systems. In its original sense, integrability means that a system of equations can be solved by quadratures. Integrability is closely linked to the existence of integrals (or constants) of motion. The integrability property depends on: 1. how many constants of motion exist; 2. how precisely they are related; 3. how the phase space is foliated by their level sets. A system of differential equations is said to be completely integrable by quadratures if its solutions can be found after a finite number of steps involving algebraic operations and integration of given functions. Integrability and chaotic motion are in some sense opposite properties of dynamical systems. But integrability is rare and exceptional, while chaotic nature is generic. There are several important examples of completely integrable mechanical systems. Here are some of them: 1. motion in Euclidean space under a central potential; 2. motion at the two Newtonian centers; 3. geodesics on a surface of a triaxial ellipsoid; 4. rigid-body motion about a fixed point; 5. the Neumann model.¹ As we shall see later, the geodesic motion of test particles and light in the gravitational field of a stationary axisymmetric black hole (described by the Kerr metric) is completely

¹This model describes the motion of N particles on S^{N-1} under the action of harmonics forces on each of them. The corresponding Lagrangian

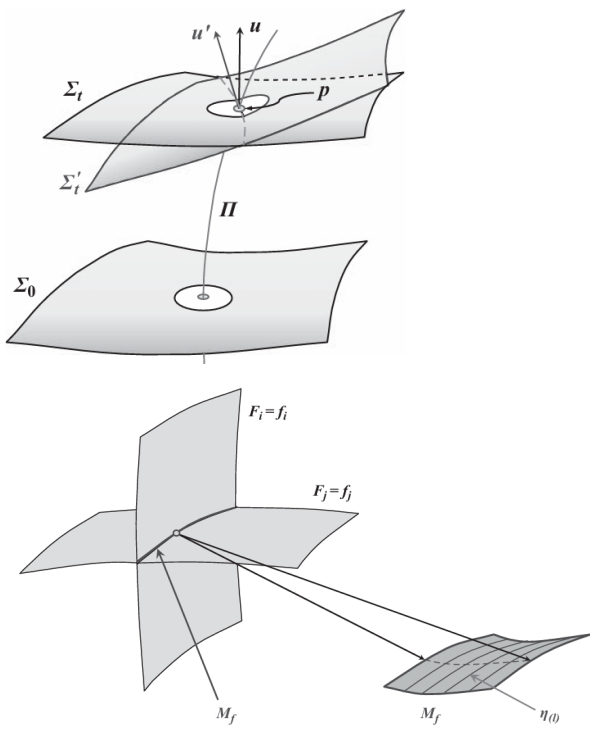
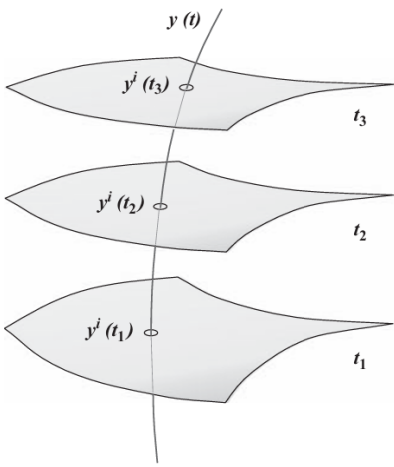


Fig. 4.6 Submanifold M_f and the Hamiltonian flux on it.

The foliation of the spacetime by a set of 3-dimensional space-like surfaces t, t_3, t_2, t_1 where the variables g_{ij} is the inverse matrix to g_{ij} .

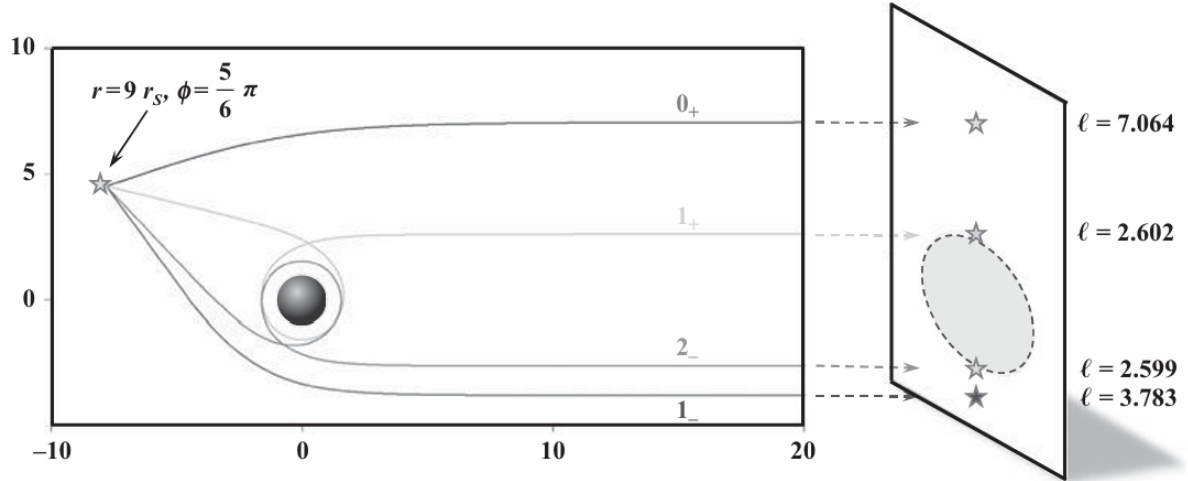


Quantum field: In the Feynman path integral approach an amplitude of a probability of a transition of a quantum system from one quantum state to another is given by the functional integral of $\exp(iS/h)$, where S is the classical action of the system. In the classical limit, when $S \gg h$, the main contribution to this integral is given by the extremum of the action. That is how the classical equations of motion follow from quantum theory.

Example: consider a term that has the structure $gn(\partial g)m(\partial^2 g)k$, where n, m and k are integer numbers. If $k > 1$ the variation of the $(\partial^2 g)k$ term would contain fourth derivatives. If $k = 1$ and $m \geq 1$ a variation of $(\partial g)m$ after the integration by parts would give terms where an extra derivative is acting on the term with the second derivative, which results in the appearance of a third derivative in the equation of motion. Thus, in order to have the second-order equations either $k = 0$ or $k = 1$ and $m = 0$.

Quantum structures(teleportation-inverse-non-rays)

Fig. 7.12 Null rays for the first four images of the object located at $= 9rS$ and angle $\phi = 5\pi/6$. Images $1+, 2-$ and all images with higher winding numbers concentrated near the critical impact parameter $= \min = 3\sqrt{3}/2$.



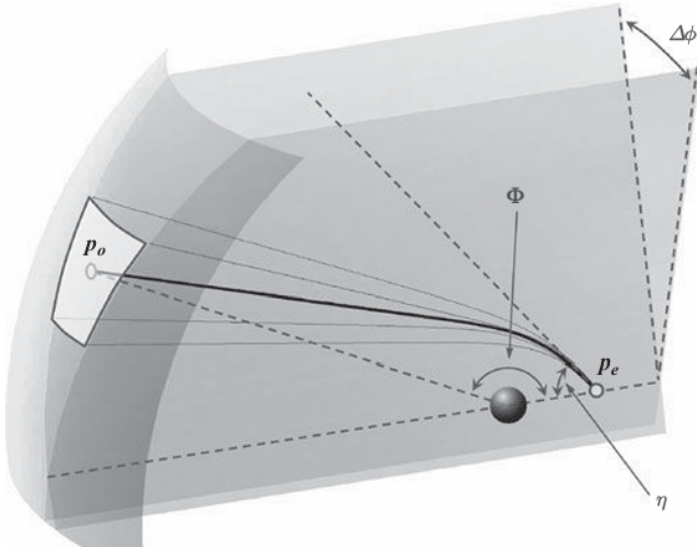
Variables and polarity signs: The sign (+) are above the black hole shadow, and images with sign (-) are below it. Using Eq. (7.4.10) or the bending angle one can write a condition that determines the inverse impact parameters for the image as follows $\pm n = \pm (\zeta e, \zeta^2) + (\zeta o, \zeta^2)$.

A Plus sign is for the case when the radial turning point is between p_e and p_o , while the sign is minus in the opposite case. For the observer located far from the black hole $r_o > r_S$, so that $\zeta o < 1$. In the leading-order approximation we put $\zeta o = 0$ in Eq. (7.6.8) $\pm n = \pm (\zeta e, \zeta^2), \pm (\zeta, \zeta^2) = \pm (\zeta e, \zeta^2) + (0, \zeta^2)$.

Figure 7.13 shows the plot of $\pm(\zeta, \zeta^2)$ as a function of ζ^2 for a fixed value of ζ . To find the parameter ζ^2 that specifies the null ray, one needs to solve Eq. (7.6.8). It's easy to see that for all the rays, except the primary one, the branch $-$ does not give solutions, so that for $n > 0$ the equation is $2\pi n \pm = +(\zeta, \zeta^2)$, $n > 0$.

We denote its solutions by $\zeta_{n,\pm}$. The images for the sign (+) are seen on the same side of the black hole as the primary image, while the images corresponding to the sign (-) appear on the other side of the black hole. The Figure 7.12 schematically illustrates these images.

$\eta = \eta_{n,\pm}(\zeta)$, (6.12) 7. where $(n\pm)$ is the index enumerating the rays. Consider Solid angle with the tip at the black hole and restricted by spherical coordinates $\theta \in (-\pi/2, +\pi/2)$, $\varphi \in (-\varphi/2, \varphi/2)$.



One way to consider equations is as a dimension or higher-dimensional structure, where quantum rays are merged along the curvature of a black hole. This representation can also be depicted as a quantum circuit, akin to a hologram or a dark matter-related quantum light-laser.

The aperture A of telescope at p_o can be expressed in terms of the solid angle $A = r^2 \Omega$, $\Omega = |\sin \eta| \Omega \varphi$.

Geodesics- -quantum rays, geodesics, quantum circuits:

The null geodesics relates the angle η of the emitted ray and angular coordinate of the telescope .This gives the condition the range of angles of the emitted rays that reach the telescope: $\eta = \eta(\alpha) \pm \eta/2$,where $|\eta| = d\eta(\alpha) d\alpha$. The brightness of a particular spectral line is proportional to the specific flux F_v of photons of the given frequency emitted by the source that reaches the observer.

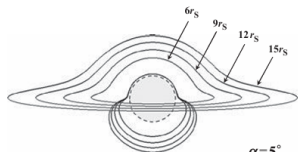


Fig. 7.20 Images of the four circular orbits for the angles $\alpha = 5^\circ$.

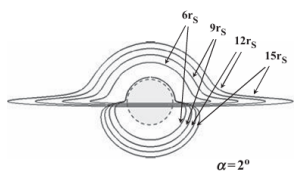
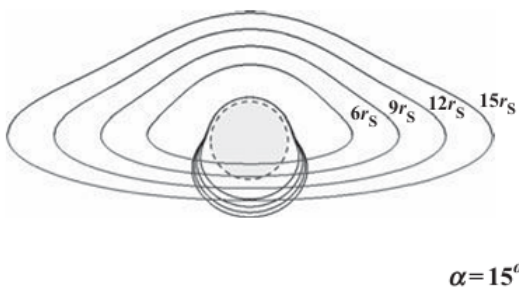
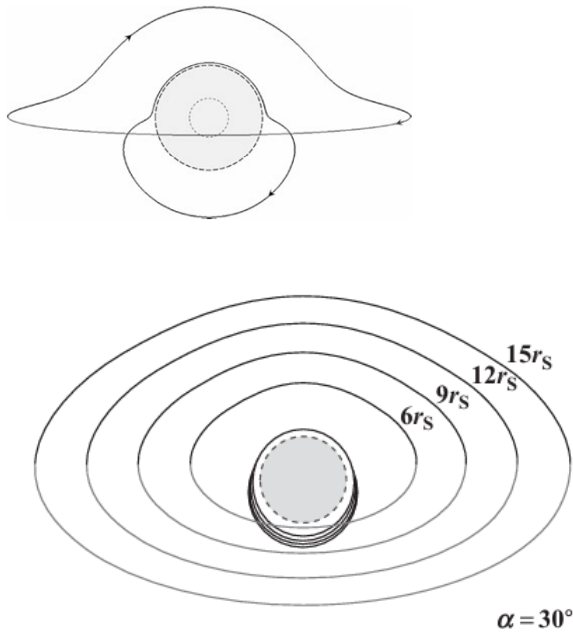


Fig. 7.21 Images of the four circular orbits for the angles $\alpha = 2^\circ$.

Orbits: the circular orbit at radius $r = 9r_s$ as seen from the angle $\alpha \equiv \pi/2 - \iota = 50$ to the orbit.



Radiation and quantum circuits:

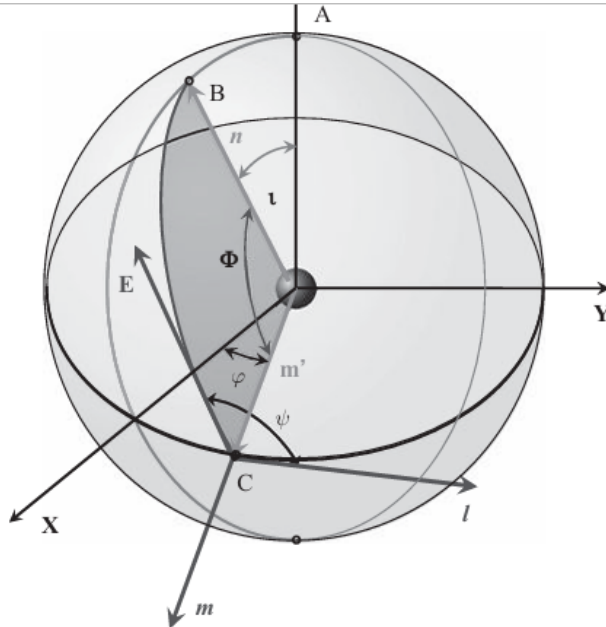
Fig. 7.22 Radiation from a source moving along a circular Keplerian orbit around a Schwarzschild black hole. A Unit sphere the figure corresponds to the 2d Section (θ, φ) of the spacetime. It also shows different angles that are used in this problem.

Radiation problem:

For $\tau = 0$ this problem is quite similar to one discussed in the previous subsection. Additional problems that arise for $\tau = 0$ are two kinds: 1. more involved relations between the direction of emitted null rays that reach the observer; 2. time dependence of the position of the point of emission.

We draw a sphere unit radius with the internal geometry $d\omega^2 = d\theta^2 + \sin^2\theta d\varphi^2$.

To the distant observer is in the (X,Z)-plane, and denotes a unit vector in this direction by n . The endpoint of this vector on the unit sphere is at the point B. We define the inclination angle ι by the relation $\cos\iota = (n, k)$.



We Make the following simplifying assumptions: 1. We restrict ourselves by considering the primary images, so that $n = 0$. 2. We Assume that Eq. (7.7.16)for $n = 0$ and $\iota \in (\pi/2 - \iota, \pi/2 + \iota)$ has a solution.

Observer: ages. Thus, we have the following equation $A \pm \pi n = \pm(\zeta, \zeta)$.

Circuit-taxonomy in the space

We can integrate the concepts of quantum circuits into a broader mathematical framework. Our goal is to incorporate the paths, lines, and buses into a black hole's curvature to analyze and synthesize new forms of matter and energy. By leveraging holograms and observing these patterns, we can replicate the materials found in magnetars or other cosmic entities. This process involves mimicking the structural properties of Riemannian tensors within quantum circuits, thereby advancing quantum technology to create new fuels, machinery, and circuits inspired by celestial phenomena.

Python Script with Qiskit Metal

Here is a basic script to get you started with Qiskit Metal, focused on creating quantum circuits with a 5-dimensional approach:

```
import numpy as np
from qiskit import QuantumCircuit, transpile
```

```

from qiskit.visualization import plot_histogram
from qiskit.providers.aer import AerSimulator

# Define a 5-dimensional quantum circuit
num_qubits = 5
qc = QuantumCircuit(num_qubits)

# Apply Hadamard gates to all qubits
for qubit in range(num_qubits):
    qc.h(qubit)

# Apply CNOT gates in a loop to create entanglement
for qubit in range(num_qubits - 1):
    qc.cx(qubit, qubit + 1)

# Apply a black hole inspired curvature (represented by rotation
gates)
curvature_factor = np.pi / 4 # Example value, adjust as needed
for qubit in range(num_qubits):
    qc.rz(curvature_factor, qubit)

# Measure all qubits
qc.measure_all()

# Simulate the circuit
simulator = AerSimulator()
compiled_circuit = transpile(qc, simulator)
result = simulator.run(compiled_circuit).result()
counts = result.get_counts()

# Plot the results
plot_histogram(counts).show()

print("Quantum circuit with 5-dimensional approach and black hole
curvature applied.")

```

Vector propagation

We Choose the flat coordinates (X,Y,Z) in E3 so that the dimensional plane of the orbit coincides with the (X,Y)-plane. Unit vector k along the axis of rotation is directed along Z. We choose the 226 Particles and Light Motion in Schwarzschild Spacetime coordinates so that the direction to the distant observer is in the (X,Z)-plane, and denote a unit vector in this direction by n. The endpoint of this vector on the unit sphere is at the point B. We define the inclination angle ι by the relation $\cos\iota = (n, k)$.

“The transformation of our perspective involves comparing images of a quantum circuit and signal detection with an FPGA, and making the circuit behave or imagining how it would behave in the context of stellar rays within the structure of a black hole. This represents the future of a new type of space station”

Circuits:

Circuit Configuration: We define a quantum circuit with 5 qubits.

Hadamard Gates: We apply Hadamard gates to all qubits to create superposition.

Entanglement: We use CNOT gates to entangle the qubits. **Black Hole Inspired Curvature:** We apply rotation gates (RZ) with a curvature factor inspired by black holes. **Measurement:** We measure all the qubits and simulate the circuit.

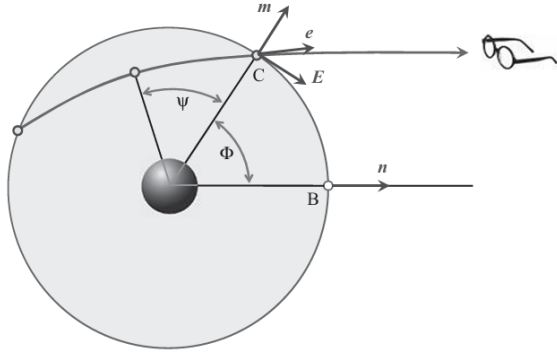


Fig. 7.23 Null-ray orbit in the 2D plane (r, Φ) .

Conclusion

This summary explains in simple terms that it is possible to integrate quantum circuit technology and quantum algorithms, like those from CERN, into larger scales or dimensions, such as 4D or 5D. It suggests that within a billion years, humanity may have invented an object that mimics the curves of a black hole and behaves according to the principles of quantum algorithms and vectors. This highlights the potential for groundbreaking advancements in quantum technology and our understanding of the universe.

Some type of space station is represented as a tetrahedron or higher-dimensional shape, adapting to the speeds of light within our galaxy to address an existing gap: the current impossibility of traveling to other galaxies.

Symbols: (+) corresponds to the rays that include the radial turningpoint, while (-) corresponds to the rays that do not reach the turning point. In order to reach the observer the corresponding bending angle for the ray must be equal to or $\pm n\pi$ for higher-order images. Thus, we have the following equation $\pm n\pi = \pm(\zeta_1\zeta_2)$. For the given radius of the orbit the parameter ζ is fixed. For the given angle (7.7.16) and the winding number n this equation determines the position of the turning point ζ_2 and, hence, the impact

parameter of the null ray. We Make the following simplifying assumptions: 1. We restrict ourselves by considering the primary images, so that $n = 0$. 2. We Assume that Eq. (7.7.16) for $n = 0$ and $\in (\pi/2 - \iota, \pi/2 + \iota)$ has a solution.

Circuit integration(buses-qubits)

The second condition means that the inclination angle is not too close to $\pi/2$. If the angle $\pi/2 - \iota$ is small there exist primary rays with the impact parameter $< \min$. The rays from this part of the orbit arrive in the blackhole shadow domain. This case requires separate consideration with small modifications. We Denote the solution ζ_2 of the equation $= \pm(\zeta, \zeta_2)$

Particles and Light Motion in Schwarzschild Spacetime as a quantum circuit(idea)

For every point C on the orbit one can calculate the null geodesic connecting it to the observer at infinity. The corresponding inverse impact parameter $q(t)$. From now on we shall consider vectors in the 4D spacetime, Denote $e^t = (g-1/2, 0, 0, 0)$, $e^r = (0, g1/2, 0, 0)$, $e^\varphi = (0, 0, 0, R-1) = (0, 0, R-1l)$, $k = (0, 0, R-1E)$.

We denote by u the 4-velocity of the Keplerian Motion in the equatorial plane $u = \gamma(e^t + v e^\varphi) = (\gamma g-1/2, 0, 0, R-1v\gamma)$.

The momentum p of the emitted null ray at the point of emission one has $p = \lambda(e^t + \alpha e^r + \beta k)$.

Frequency-emission: For the emitted frequency ω_0 , measured in a frame moving with the body, one has $\omega_0 = -(u, p) = \lambda\gamma(1 - \beta v \cos\psi)$.

Basic ideas:

The main new features for the charged particle motion near a magnetized Schwarzschild black hole are:

1. No trajectory can reach infinity.
2. A Particle is either finally trapped by the black hole, or is bounded.
3. The radius of the innermost stable circular orbit becomes smaller and for $b \rightarrow \infty$ and > 0 it reaches r_S .
4. Bounded non-circular orbits can be either ‘smooth’, or ‘curly’. The type of motion depends on the amplitude of radial oscillations.
5. A Critical trajectory, separating these two different cases, has cusps.
6. The action of the gravitational field generates drift current

Pseudocode-comparison in trajectories:

```
Algorithm II-QIPM
Input: Initial guess for variables, maximum iterations
Output: Optimized variables
```

```

Initialize variables
While not converged and iterations < max_iterations do
    Solve Newton system (Eqs. (19) and (22))
    Update variables
    Check for convergence
End while

```

Algorithm IF-QIPM

```

Input: Initial guess for variables, maximum iterations
Output: Optimized variables

```

```

Initialize variables
While not converged and iterations < max_iterations do
    Solve Newton system (Eqs. (23) and (24))
    Update variables
    Check for convergence
End while

```

Algorithm IF-QIPM-QR

```

Input: Initial guess for variables, maximum iterations
Output: Optimized variables

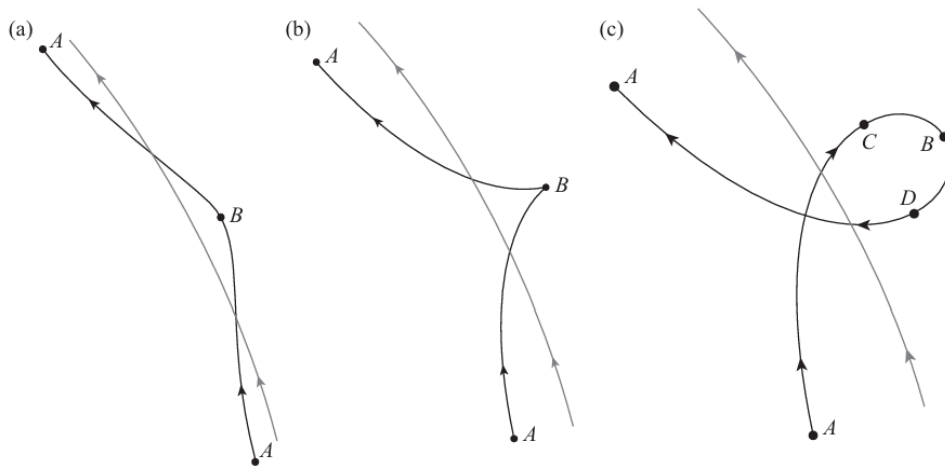
```

```

Initialize variables
While not converged and iterations < max_iterations do
    Perform classical QR decomposition
    Solve Newton system with QR decomposition (Eqs. (23) and
(24))
    Update variables
    Check for convergence
End while

```

Fig. 7.25 Types Of Bounded Trajectory Corresponding To $\epsilon > 0$. The Figure Show Segments Of Trajectories for 3 different types of motion, discussed in the text. Arrows illustrate the direction of motion of charged particles. Circular arcs represent the stable circular orbit defined by $\rho = \rho_{\min} +$



7.10.1 Equation of motion and properties of particle and light motion in the gravitational field of a D-dimensional non-rotating black hole. The corresponding metric is (see Eq. (6.8.2)) $ds^2 = -g dt^2 + dr^2 g + r^2 d\omega^2 D-2$, $g = 1 - (r_s/r)^D - 3$. (.1)

The problem of isometric embedding of 2D manifolds in E3 is well studied. It is known that any compact surface embedded isometrically in E3 has at least one point of positive Gauss curvature. Any 2D compact surface with positive Gauss curvature is always isometrically embeddable in E3, and this embedding is unique up to rigid rotations. (For a general discussion of these results and for further references, see, e.g., (Berger 2003).) For the embedding of a 2D surface into the Euclidean space E3 there exists a simple relation between the Gaussian curvature K and the extrinsic curvature Kab ($a, b = 1, 2$), $K = 1/(K_2 - K_{ab}K^{ab})$.

Equations:

Matrix Kab: We define the diagonal matrix Kab with k1 and k2.

Equation (2.35): Displays the diagonal matrix Kab.

K2 Calculation: Computes $K_2 = (k_1 + k_2)^2 / 2$.

Equation (2.36): Computes $KabKab = k_{12} + k_{22}$.

Equation (2.37): Computes $K = k_1 \times k_2 / (k_1 + k_2)$.

Cylindrical Coordinates: Defines a function to calculate the distance $dL2dL2$ in 3D Euclidean space using cylindrical coordinates.

```
import numpy as np

# Define the diagonal matrix Kab
k1 = 1.0 # example value
k2 = 2.0 # example value
Kab = np.diag([k1, k2])

# Equation (2.35)
print("Kab:")
print(Kab)
```

```

# Calculate K2
K2 = (k1 + k2)**2
print("K2:")
print(K2)

# Equation (2.36)
KabKab = k1**2 + k2**2
print("KabKab:")
print(KabKab)

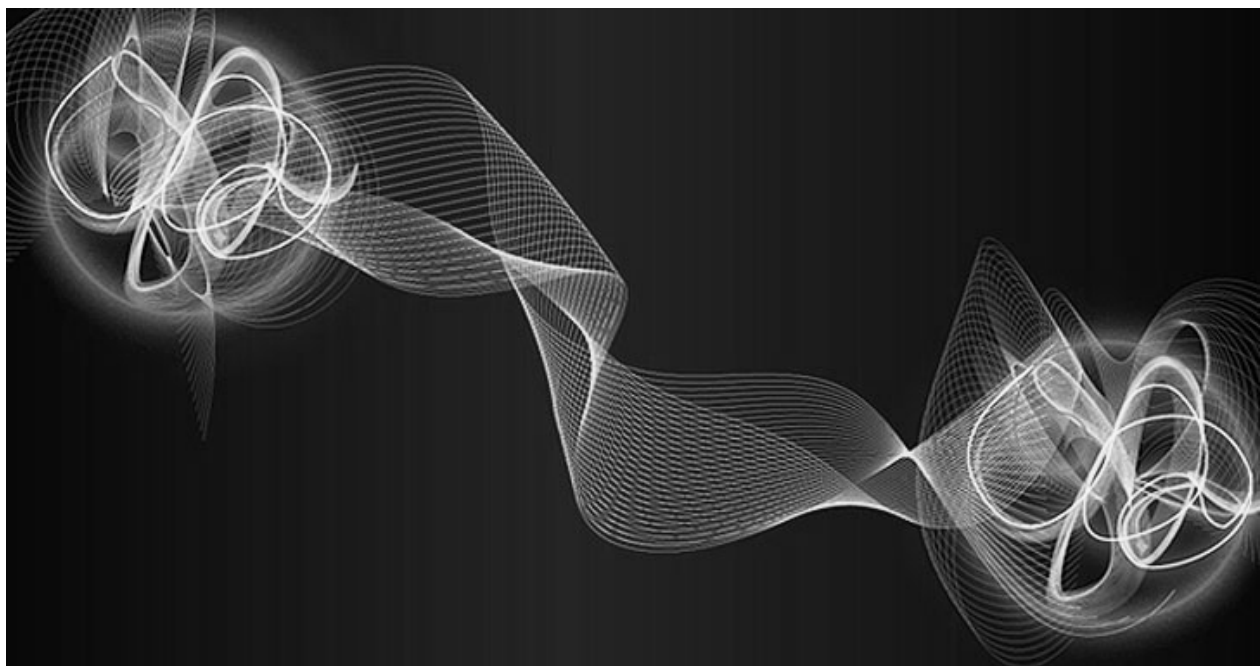
# Equation (2.37)
K = k1 * k2
print("K:")
print(K)

# For axisymmetric distorted 2D spheres in 3D Euclidean space in
cylindrical coordinates
def cylindrical_coordinates(dZ, dRho, dPhi):
    dL2 = dZ**2 + dRho**2 + (dRho**2 * dPhi**2)
    return dL2

# Example values for the coordinates
dZ = 1.0
dRho = 1.0
dPhi = np.pi / 4 # 45 degrees in radians

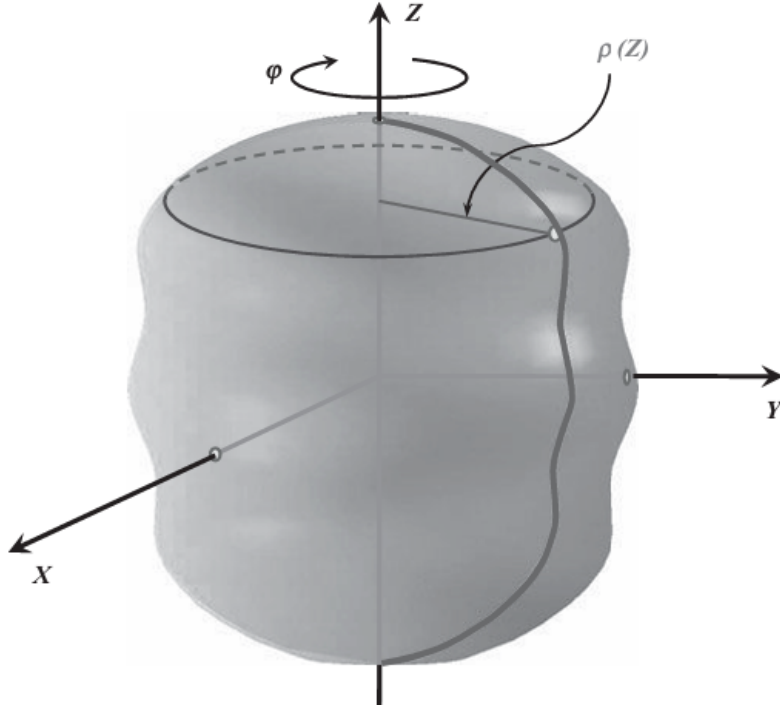
dL2 = cylindrical_coordinates(dZ, dRho, dPhi)
print("dL2 (cylindrical coordinates):")
print(dL2)

```



Choose a line $\rho = \rho(Z)$ at fixed ϕ and rotate it in the ϕ -direction around the Z -axis. The obtained surface is called a *revolution surface* (see Figure 8.1). The induced 2D geometry on it is

$$dS^2 = [1 + (d\rho/dZ)^2] dZ^2 + \rho^2 d\phi^2. \quad (8.2.39)$$



Temperature & curvature: The detailed information about the local observables can be obtained if one knows the thermal Green function. In the case of the thermal radiation in the Rindler spacetime this Green function can be found in an explicit form. Consider The Euclidean Rindler space $ds^2 = a^2 \rho^2 d\tau^2 - E + d\rho^2 + dy^2 + dz^2$, (9.8.14) and impose the periodicity condition on the Euclidean time τE . Namely, we assume that the length circle $\rho = a - 1$ is β . In the general case, space has a cone-like singularity at $\rho = 0$. The corresponding embedding diagram for the 2D (τ, ρ) -section is shown in Figure 9.8. The singularity is absent only when $\beta = 2\pi/a$. (9.8.15) For quantum field theory the periodicity in the imaginary time corresponds to the thermal state with the temperature $T = \beta^{-1}$. In the absence of the conical singularity the temperature T is $a = 2\pi\beta$. This is called the Unruh temperature.

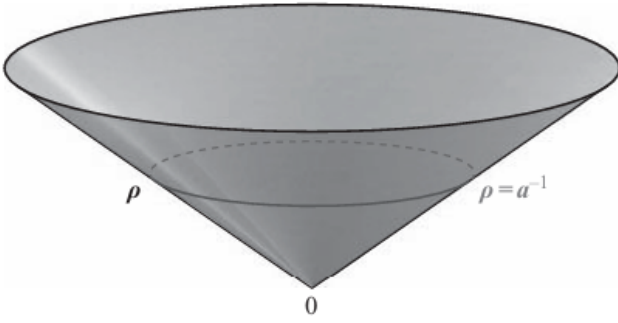


Fig. 9.8 The embedding diagram for 2D (τ, ρ) -section of the Euclidean Rindler space.

9.8.3 Thermal Green functions Consider the thermal radiation in the Rindler space. The outgoing thermal flux from the Rindler horizon, being reflected back by the potential, generates the incoming flux. The combination of these two fluxes results in thermal equilibrium state. Since in an external gravitational field the local temperature depends on the position, one needs to choose a special normalization point for its identification. We use $\rho = a-1$ as such a point and denote by 0 the temperature there

Explanation of the Pseudocode

1. **dF Function:** Computes the distance metric based on the provided formula.
2. **N Function:** Determines whether a point lies within the neighborhood $N(\gamma)N(\gamma)$ based on the distance metric.
3. **NF Function:** Checks if a point is within the feasible neighborhood $NF(\gamma)NF(\gamma)$ by ensuring it is both in $N(\gamma)N(\gamma)$ and feasible.
4. **Iterate Points:** Iteratively checks and updates points within the neighborhood. Uses the Newton system to find the next point and ensures each intermediate point lies within $NF(\gamma)NF(\gamma)$.

This pseudocode lays out the basic structure for managing a 5-dimensional metric space and handling points within specified neighborhoods

```
# Pseudocode to define a 5-dimensional metric space and determine neighborhoods

# Function to compute dF
function dF(x, tau, s, k):
    mu = mu(x, tau, s, k)
    return sqrt(2 * (T * x * s - mu) + (tau * k - mu)**2)

# Function to determine neighborhood N
function N(y, x, y, tau, theta, s, k):
    mu = mu(x, tau, s, k)
    distance = dF(x, tau, s, k)
```

```

if distance <= γ * mu:
    return True
else:
    return False

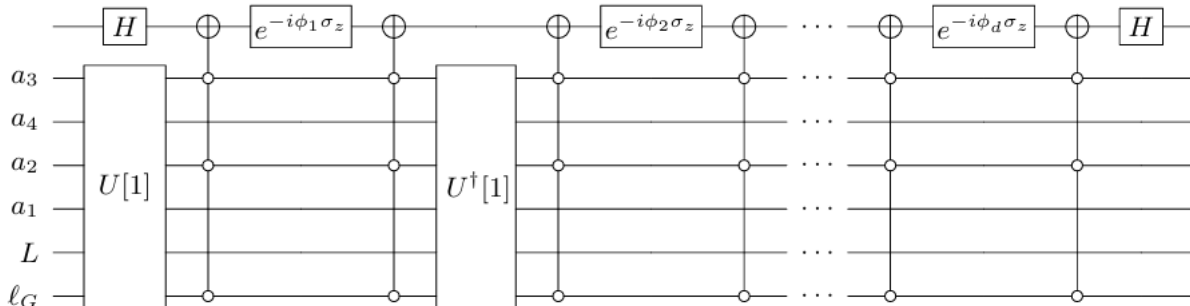
# Function to determine feasible neighborhood NF
function NF(γ, x, y, τ, θ, s, κ):
    if N(γ, x, y, τ, θ, s, κ) and is_feasible(x, y, τ, θ, s, κ):
        return True
    else:
        return False

# Main routine to iterate and check points
function iterate_points(γ, max_iterations, initial_point):
    (x, y, τ, θ, s, κ) = initial_point
    for i from 1 to max_iterations:
        if NF(γ, x, y, τ, θ, s, κ):
            (x_new, y_new, τ_new, θ_new, s_new, κ_new) =
next_point(x, y, τ, θ, s, κ)
            if NF(γ, x_new, y_new, τ_new, θ_new, s_new, κ_new): # check with updated γ value
                (x, y, τ, θ, s, κ) = (x_new, y_new, τ_new, θ_new,
s_new, κ_new)
            else:
                break

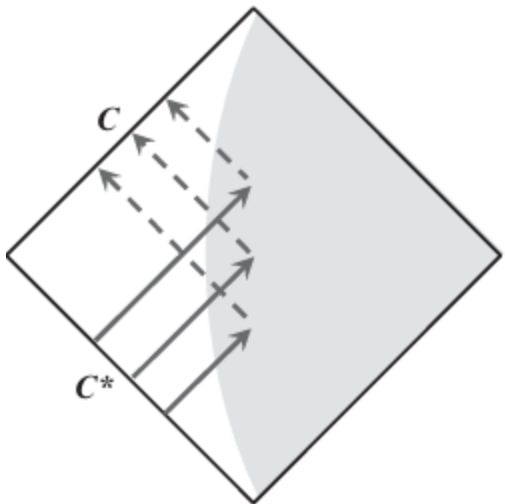
# Example values
γ = 1/10
σ = 1 - (20 * sqrt(2) * sqrt(r + 1))**(-1)
max_iterations = 100
initial_point = (x_init, y_init, τ_init, θ_init, s_init, κ_init)

iterate_points(γ, max_iterations, initial_point)

```



Quantum circuit, we have to integrate the circuit variables and quantum relations.events into the curvature of the black hole step before creating a new space object inspired on quantum behavior and the black hole behavior.



V. IPM IMPLEMENTATION AND RESOURCE ESTIMATES FOR PO IN BLACK HOLE CURVATURE/QUANTUM MECHANICS-BLACK HOLE TOPOLOGIES

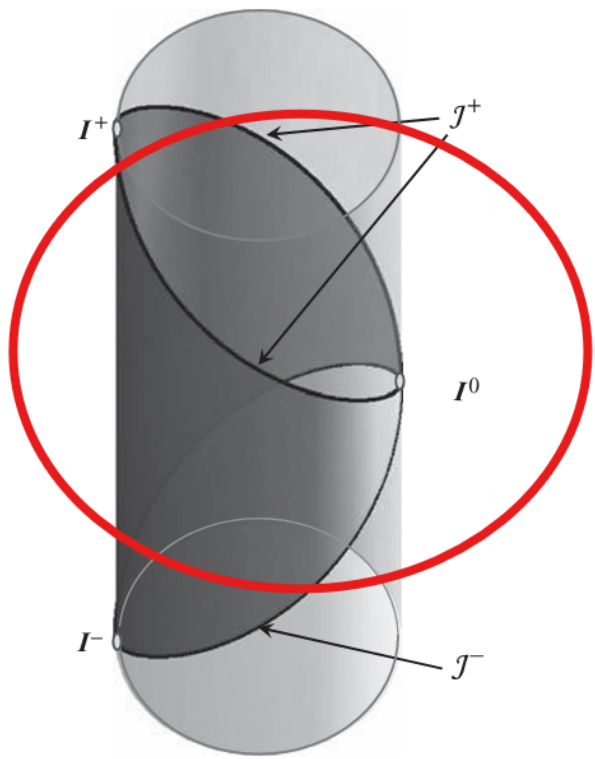
Factors in high order topologies (circuits-blackholes)

The conformal factor $=2\cos 1/2(\psi + \xi)\cos 1/2(\psi - \xi)$. (10 vanishes at the ‘boundary’ of the Minkowski spacetime. This boundary consists of the following pieces:

Surface of the Quantum boundaries & black holes (oscillators, compressors in the 3D-4D)

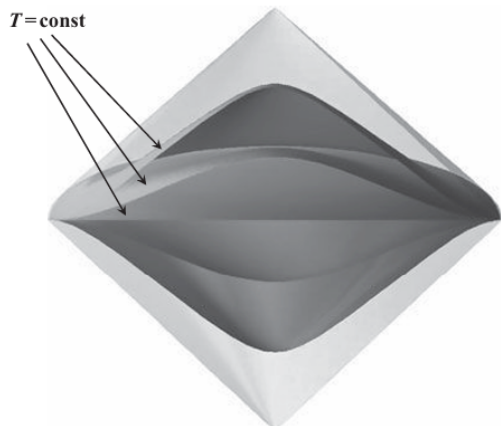
1. The past null infinity $J-$, where $\psi = -\pi + \xi$ and $0 < \xi < \pi$. 2. The future null infinity $J+$, where $\psi = \pi - \xi$ and $0 < \xi < \pi$. These Boundaries Are Null surfaces in the metric $d\tilde{s}^2$. 3. The spatial infinity I^0 where $\xi = \pi$. I^0 4. The future, I^+ , and the past I^- time-like infinities, where $\psi = \pi$ and $=-\pi$,respectively. The coordinate transformation Eq. (10.1.5) is chosen so that it brings the points of infinity to the finite coordinate ‘distance’. Points at infinity in the Minkowski spacetime correspond to $\psi + \xi$ and $\psi - \xi$ with the values $\pm\pi$.At these values, the metric ds^2 becomes meaningless, but the metric $d\tilde{s}^2$, conformal to ds^2 , is regular 1. At a Fixed Value of ψ the metric Eq. (10.1.7) is $d\tilde{l}^2 = d\xi^2 + \sin^2 \xi d\omega^2$.

Equations $\psi \pm \xi = \text{const}$ give null lines. A shadowed region is an image of the Minkowski spacetime. To illustrate the properties of the Minkowski spacetime in the new coordinates we consider its 3D section $Z = 0$. On this section $\theta = \pi/2$ and the line element is $ds^2 = -dT^2 + dR^2 + R^2 d\phi^2 = 2d\tilde{s}^2$, $d\tilde{s}^2 = -d\psi^2 + d\xi^2 + \sin^2 \xi d\phi^2$.



Coordinates-map: the coordinate domain for (ψ, ξ, φ) . We choose ξ as a radial coordinate, and φ is the corresponding polar angle. Let us Emphasize that these figures are not embedding diagrams. We use them to illustrate the coordinates from different surfaces and lines of the original Minkowski spacetime.

Circuit-Map: Holograms, spatial stations which adapts to a black hole topologies and also quantum resources are critical in this research:



```
plt.show() # Print  $\psi$  and  $\xi$  to inspect their values print(  
# Print  $\psi$  and  $\xi$  to inspect their values print(f' $\psi$ : {psi}') print(f' $\xi$ : {xi}')
```

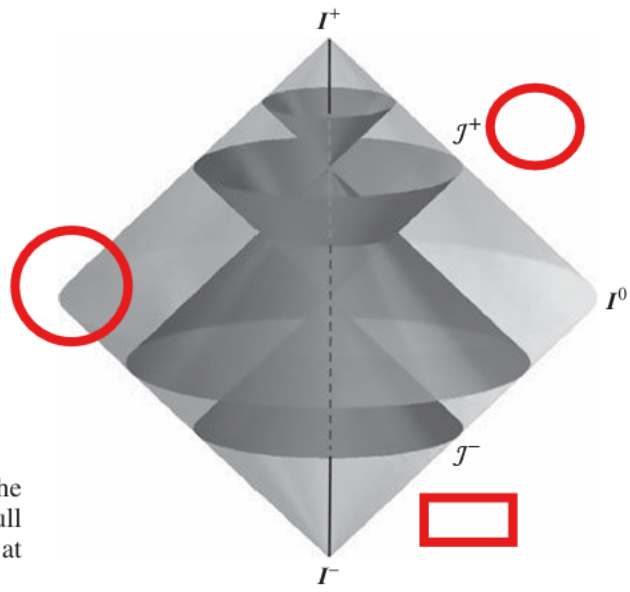
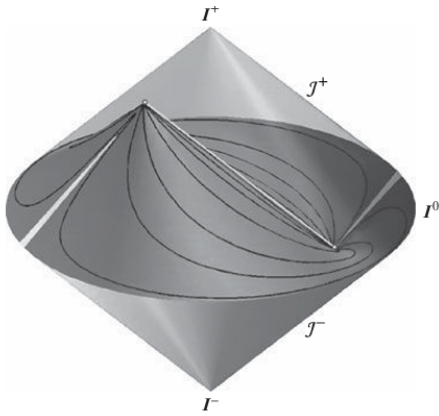


Fig. 10.4 Carter-Penrose diagram of the Minkowski spacetime. This figure shows null cones passing through the origin $R = 0$ at different moments of time T .

Coordinates: the direction of the X-axis and passing through $X = 0$. Its equation is $T = X$. We call a null line $Y = b$ on this plane a generator and b its impact parameter. Let us find the equation of the null plane in the (ψ, ξ, ϕ) coordinates.

Analysis with python:

```
import numpy as np
import matplotlib.pyplot as plt
# Define the range for phi
phi = np.linspace(-np.pi / 2, np.pi / 2, 1000)
# Define constant b
b = 1
# Adjust as needed
# Calculate R, X, Y
R = b / np.cos(phi)
X = b * np.tan(phi)
Y = b
# Calculate W+ and W-
W_plus = b * (np.sin(phi) + 1) / np.cos(phi)
W_minus = b * (np.sin(phi) - 1) /
```



Analysis (formal)

The surface $T = X$ and its generators are shown in Figure 10.5. One can see that all the null generators start from a single point of the J^- and end at a single point of the J^+ . The basic generator $b = 0$ is a straight line going through J^- to J^+ and passing through the origin $\xi = 0$. Problem 10.1: Let η be a null geodesic in the

metric $g_{\mu\nu}$. Show that after a conformal transformation of variables across the given values $g_{\mu\nu} = 2 - g_{\mu\nu}$ it remains a null geodesic in the conformal metric $\tilde{g}_{\mu\nu}$.

We have already mentioned that at the ‘boundary’ the conformal factor However, its gradient is finite at $J\pm$. In the coordinates $(\psi, \xi, \theta, \phi)$ one has $,\mu J+ = -\sin\xi \cdot (1, 1, 0, 0)$, $,\mu J- = \sin\xi \cdot (1, -1, 0, 0)$. vanishes. (10.1.17) The vectors μ are regular null vectors on $J\pm$, tangent to these surfaces.

Python simulates the concept of Bionic Object traveling at Light speed:

```

import numpy as np

# Key Variables
v = 0.9 * 3e8 # Speed of QBO in meters per second (0.9c)
c = 3e8         # Speed of light in meters per second
d = 2.537e6 * 9.461e15 # Distance to Andromeda in meters
                        # (light-years to meters conversion)

# Time Dilation Factor
gamma = 1 / np.sqrt(1 - (v/c)**2)

# Effective Time Experienced by QBO
t_prime = d / (v * gamma)

# Print results
print(f"Speed of QBO (v): {v} m/s")
print(f"Distance to Andromeda (d): {d} meters")
print(f"Time Dilation Factor (\gamma): {gamma}")
print(f"Effective Time Experienced by QBO (t'): {t_prime} seconds")

# Additional Concepts
# Curvature of Space-Time: Modeled by general relativity equations
# Quantum Resources: Described by quantum mechanics principles
# Gravitational Effects: Influenced by relativistic physics
# Navigational Coordinates: Determined by astronomical data

# Example calculation for \psi and \xi if needed
# W_plus = b * (np.sin(phi) + 1) / np.cos(phi)
# W_minus = b * (np.sin(phi) - 1) / np.cos(phi)
# psi = np.arctan(W_plus) + np.arctan(W_minus)
# xi = np.arctan(W_plus) - np.arctan(W_minus)

```

Concept: Quantum Bionic Object Traveling at Light Speed Through the Milky Way

Imagine a highly advanced space station constructed from materials that can manipulate and align with the curvature of black holes and access higher-order dimensions. This station, equipped with quantum resources, houses quantum objects and circuits designed for faster-than-light travel.

The goal is to send a quantum bionic object (QBO) on a journey through our Milky Way galaxy, traveling at a velocity approaching the speed of light (approximately 0.9c, as mentioned by Brian Cox), to eventually reach a marginal boundary point and enter the Andromeda galaxy.

Here's a breakdown of the key variables and the realistic scenario:

Key Variables

1. **Speed of the Quantum Bionic Object (QBO):** $v \approx 0.9c$
2. **Distance to Andromeda:** $d \approx 2.537 \times 10^6$ light-years
3. **Time Dilation Factor:** $\gamma = 1 - (v/c)^2$
4. **Effective Time Experienced by QBO:** $t' = dv \cdot \gamma t = \frac{d}{v} \cdot \gamma$
5. **Curvature of Space-Time:** Affected by the presence of black holes and higher-order dimensions
6. **Quantum Resources:** Energy states, entanglement, and decoherence
7. **Gravitational Effects:** Influence of gravitational waves and fields
8. **Navigational Coordinates:** Star charts and spatial coordinates within the Milky Way and Andromeda

Scenario

1. **Launch:**
 - The QBO is launched from the space station, utilizing quantum propulsion systems that leverage entangled particles for near-instantaneous acceleration to 0.9c.
2. **Journey Through the Milky Way:**
 - As the QBO travels, it must navigate around massive celestial bodies such as stars and black holes, using higher-order dimensions to "shortcut" through space-time.
 - The presence of black holes creates gravitational wells that the QBO can use to slingshot and maintain its velocity without expending excessive energy.
3. **Quantum Stabilization:**
 - Quantum circuits onboard the QBO continuously adjust its trajectory, compensating for any quantum decoherence and maintaining entanglement with the space station for real-time communication.
 - The QBO's internal time (t') is significantly dilated due to its high velocity, allowing it to experience a shorter travel time compared to an observer on Earth.
4. **Approaching Andromeda:**
 - As the QBO reaches the marginal boundary between the Milky Way and Andromeda, it begins to decelerate and aligns its trajectory to enter the new galaxy.
 - Quantum sensors detect gravitational waves and spatial anomalies, ensuring a safe passage into Andromeda.
5. **Arrival and Data Transmission:**
 - Upon reaching its destination, the QBO collects and transmits data back to the space station, providing valuable insights into the intergalactic space and the Andromeda galaxy.

This scenario blends advanced quantum mechanics, relativistic physics, and theoretical concepts to create a plausible depiction of a quantum bionic object traversing the vast distances between galaxies. It highlights the interplay between cutting-edge technology and the fundamental laws of the universe.

Conformal Map Summary

Step 1: Coordinate Transformation

- Brings the coordinate infinity of the Minkowski spacetime to a finite coordinate volume.

Step 2: Conformal Map

- Creates a new, regular "unphysical" space, $M \sim \tilde{M}$, where the original Minkowski spacetime M is a part.
- The conformal factor ensures the conformal metric $ds^2 \sim d\tilde{s}^2$ is regular at the image of "infinity".

Key Variables and Concepts

1. **Time-like Geodesics:**
 - Begin at infinite past I^-I^- and end at infinite future I^+I^+ .
2. **Null Geodesics:**
 - Propagate from past null infinity J^-J^- to future null infinity J^+J^+ .
 - Null generators of the fixed-null plane start at a single point of J^-J^- and end at a single point of J^+J^+ .
3. **Space-like Geodesics:**
 - Propagate between points of spatial infinity I^0I^0 .
4. **Null Boundary:**
 - Formed by two null cones, J^-J^- (past-directed from I^+I^+) and J^+J^+ (future-directed from I^-I^-).
 - Includes spatial infinity I^0I^0 and points $I^\pm I^\pm$.

This summary reduces the text while retaining the essential variables and concepts, providing a clear and concise explanation of the conformal map and its components.

Enhanced Concept: Quantum Flows in a Super Circuit

Imagine these conformal diagrams not just as mathematical constructs but as a blueprint for an immense super circuit or a uniquely designed space station. Picture quantum flows traversing through this colossal structure.

The corresponding conformal Carter–Penrose diagram (Figure 10.6) illustrates this concept. The coordinate and conformal transformations with the required properties are not unique. For example, one can make an additional transformation $\zeta \rightarrow \zeta \sim = f(\zeta) \sigma \rightarrow \tilde{\sigma} = f(\sigma)$, $\eta \rightarrow \eta \sim = f(\eta) \eta \rightarrow \tilde{\eta} = f(\eta)$.

Quantum Super Circuit Concept:

- **Nodes and Flows:** Visualize each point and line in the diagram as nodes and channels in a massive quantum circuit. Quantum particles and information would flow through these pathways, interacting and transforming as they move.
- **Quantum Stations:** Think of different regions in the diagram as specialized stations or hubs within a space station, each designed to harness specific quantum properties like entanglement or superposition.
- **Dynamic Transformations:** The coordinate and conformal transformations represent how quantum states can dynamically change, akin to how signals in a circuit adjust to different operations and conditions.

This imaginative view not only brings the abstract mathematical diagrams to life but also emphasizes the potential of quantum mechanics in designing futuristic technologies.

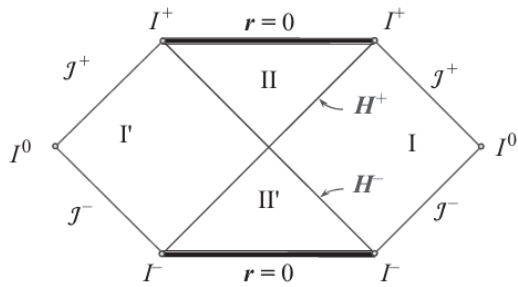
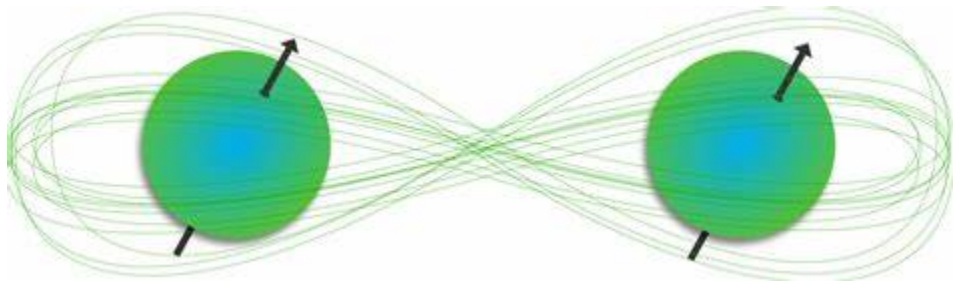
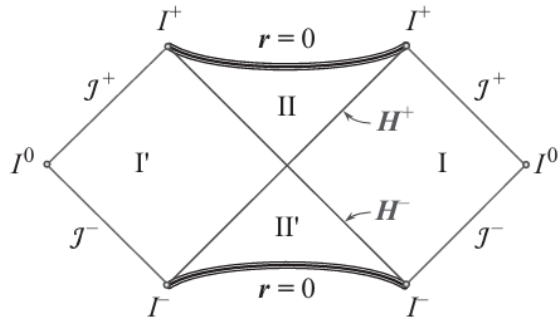


Fig. 10.7 ‘Canonical form’ of the Carter–Penrose conformal diagram. On this diagram the lines representing the singularities $r = 0$ are straightened by the additional coordinate transformation given in the text.



Metrics-space-new circuits:

A spacetime M with metric $g_{\mu\nu}$ is said to be asymptotically simple if there exists another ('unphysical') space M' with boundary $\partial M \equiv J$ and a regular metric $\tilde{g}_{\mu\nu}$ on it such that: 1. $M \setminus \partial M$ is conformal to M , and $g_{\mu\nu} = -2 \tilde{g}_{\mu\nu}$ in M ; 2. $|M| > 0$, $|\partial M| = 0$, $\mu|\partial M| = 0$; 3. each null geodesic in M begins and ends on ∂M . We call M the conformal Penrose space. Penrose prove that if the metric $g_{\mu\nu}$ satisfies Einstein's vacuum equations in the neighborhood of J (or Einstein's equations with the energy-momentum tensor that decreases to infinity sufficiently fast) and the natural conditions of causality and spacetime orientability are satisfied, then an asymptotically simple space has the following properties: 1. The topology of the space M is R^4 ; its boundary J is light-like and consists of two disconnected components $J = J^+ \cup J^-$, each with topology $S^2 \times R^1$. 2. The generators of the surfaces J^\pm are null geodesics in M ; tangent vectors to these geodesics coincide with $\tilde{g}_{\mu\nu}, \mu|J$. 3. The curvature tensor in the physical space M decreases one 'moves' along null geodesic to infinity, and the so-called peeling off property holds. Here, we don't focus on this property as its detailed analysis can be found in the literature (Sachs 1964; Penrose 1968).

Simplified Concept: Asymptotically Predictable Spacetime

Objective: To study the global causal structure of a spacetime.

Key Concepts:

1. Asymptotically Flat Spacetime:

- In such spacetimes, distant observers can see all events, represented by J^-J^+ (past) and J^+J^- (future).
- In Minkowski spacetime, J^-J^+ and J^+J^- cover the entire space, meaning no hidden regions.

2. Hidden Regions:

- In the presence of gravitating objects, there may be regions where signals cannot reach J^+J^- .
- This occurs if there is a singularity visible from infinity or a black hole.

3. Strongly Asymptotically Predictable Spacetime:

- For a spacetime $(M, g_{\mu\nu})(M, g_{\mu\nu})$ to be strongly asymptotically predictable, it must have an open region $V \subset M \setminus \tilde{V}$ $\subset \tilde{M}$ in the conformal space where $M \setminus \tilde{M}$ is globally hyperbolic, including $M \cap J^- \cap J^+ = \emptyset$.
- If a spacetime fails this condition, it is said to possess a naked singularity.

Variables

- J^-J^+ : Past null infinity.
- J^+J^- : Future null infinity.
- M : Minkowski spacetime.
- $g_{\mu\nu}$: Metric of the spacetime M .
- $M \setminus \tilde{M}$: Associated conformal space.
- $\tilde{g}_{\mu\nu}$: Conformal metric of $M \setminus \tilde{M}$.
- $V \subset M \setminus \tilde{V} \subset \tilde{M}$: Open region in the conformal space.
- Naked singularity: A singularity not covered by an event horizon.

Simplified 4D Spacetime Variables

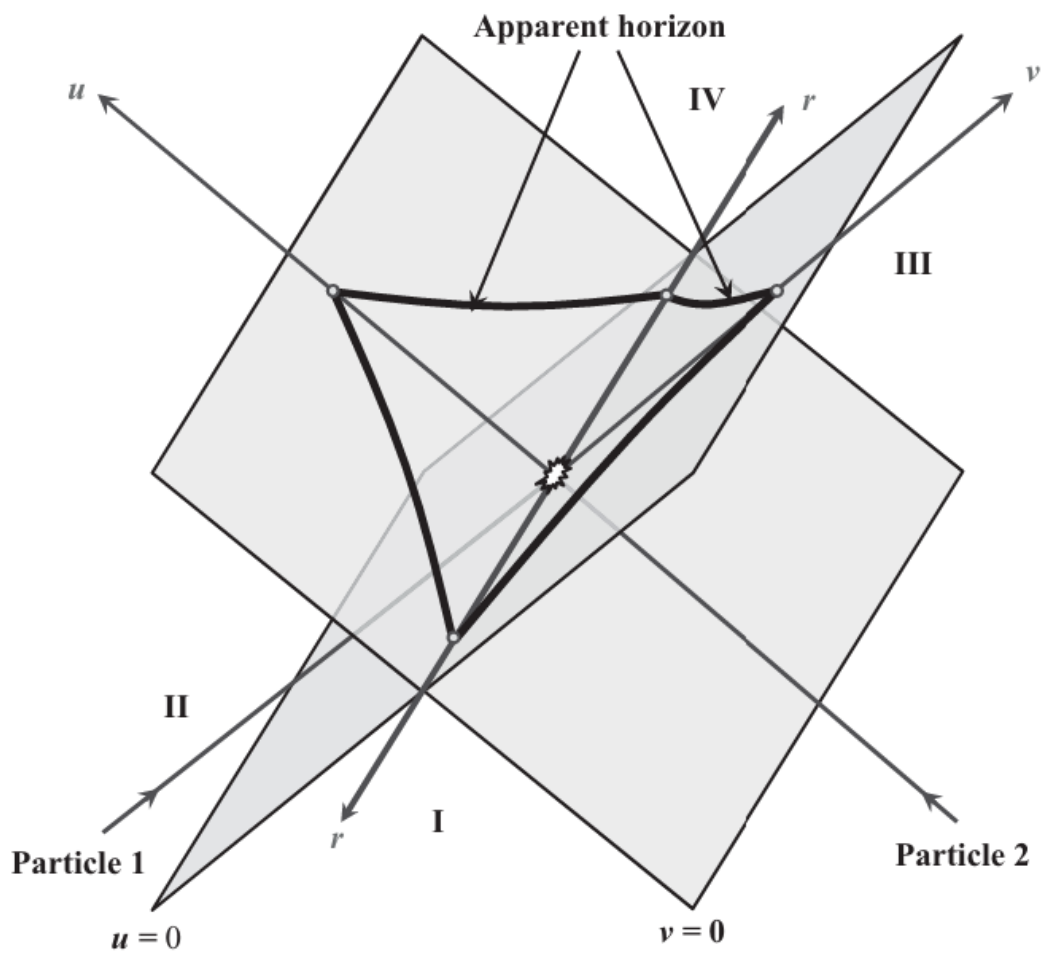
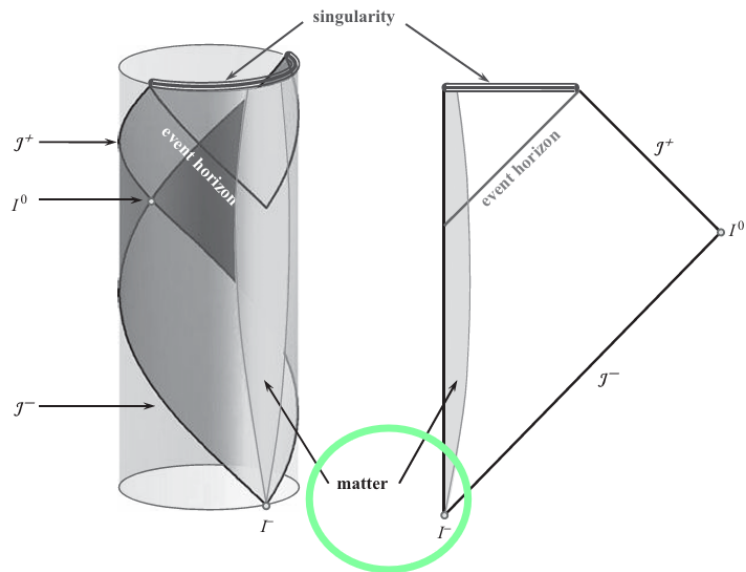
1. **Toroidal Topology:**
 - If it exists long enough, an acausal line can pass through the torus inner region from J^-J^- to J^+J^+ .
 - Such curves contradict the topological censorship theorem.
2. **Hawking Theorem Generalization:**
 - In 4D asymptotically flat stationary black hole spacetimes obeying the dominant energy condition, the event horizon cross-sections are topologically two-spheres.
 - Time-dependent cases have 2D sections BtB_t depending on foliation t .
3. **Event Horizon Geometry (Penrose 1968):**
 - Event horizon formed by null geodesics (generators) with no future endpoints.

Key Variables

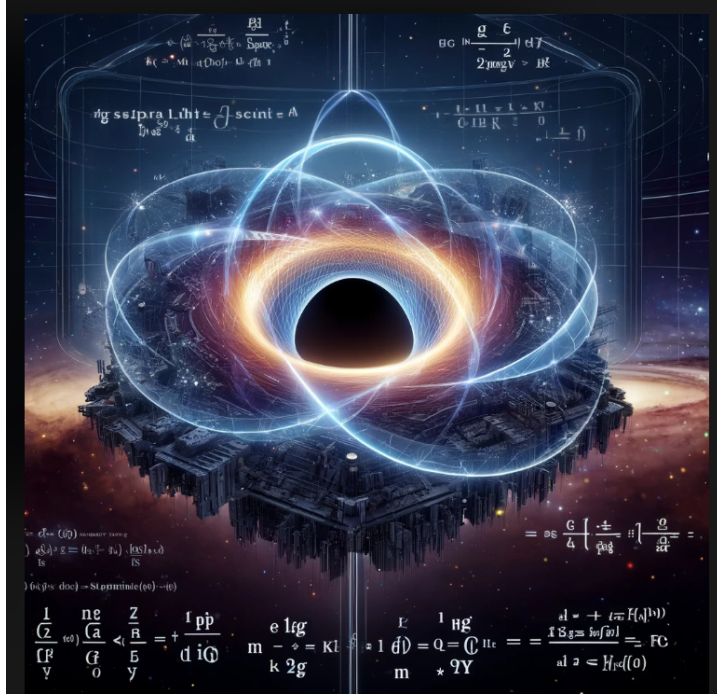
- J^-J^- : Past null infinity.
- J^+J^+ : Future null infinity.
- $\gamma_0\gamma_0$: Acausal curve.
- BtB_t : 2D sections depending on foliation t .
- Null geodesics: Paths forming the event horizon.

Types of black holes:

Primordial Black holes with mass $M \lesssim 10^{15}$ g would decay by the present time. This gives the following natural classification of the primordial black holes (PBH): 1. PBH with $M < 10^{15}$ g. These Black holes would have completely evaporated by now, but their radiation could affect many processes in the early universe. Namely, they may generate entropy, produce gravitons, neutrinos and other particles, change the details of baryogenesis. If There Exist stable relics of the Planck mass, they may contribute to dark matter. 2. PBH with $M \sim 10^{15}$ g. These black holes would have evaporated by now. The Irradiation may contribute to the Galactic γ -ray background and antiprotons and positrons in the cosmic rays. Observation of the process of their decay would give important information on the very high energy physics. 3. PBH with $M > 10^{15}$ g. These Black holes would survive till today. They may give a contribution to dark matter. Large PBHs might influence the details of the large-scale structure formation in the universe, for example serve as seeds for the supermassive black hole formation in the galactic nuclei.



Equations(quantum integration)



Let us Perform the following transformation $t = c \tilde{t} + s \tilde{z}$, $c = \cosh \alpha$, $z = s \tilde{t} + c \tilde{z}$, $s = \sinh \alpha$.

Formation of Micro Black Hole

- **Mass:** Formed black hole's mass is smaller than initial MM.
- **Energy Non-conservation:** Due to gravitational radiation propagating in the bulk, a brane observer registers energy non-conservation.
- **Collision:** Two ultra relativistic particles collide, forming a micro black hole with a small impact parameter.

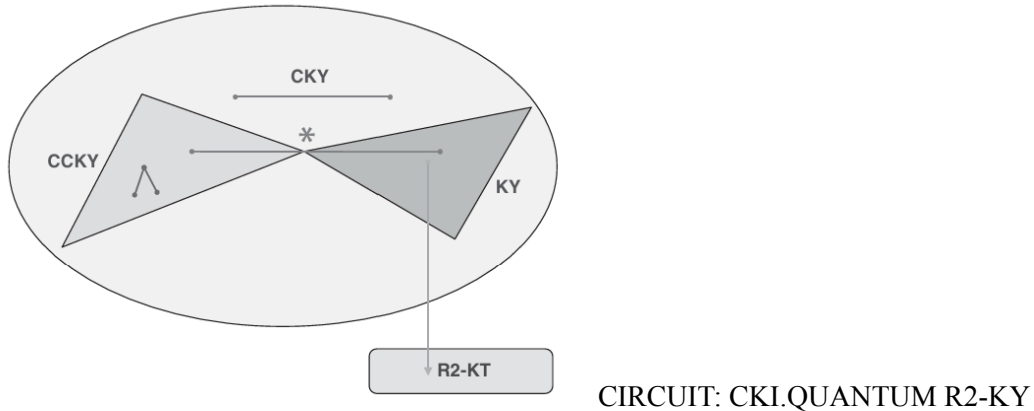
Balding Phase

- **Asymmetry:** Micro black holes are initially very asymmetric.
- **Gravitational Waves:** Emitted, leading to visible 'brane energy non-conservation'.
- **Result:** Ends as a spinning, uncharged stationary black hole.

Topology of 4D Black Hole Horizon

- **Ricci-Flat Metric:** $ds^2 = ds^2_N + r^2 d\Omega^2$ in N-dimensional spacetime.
- **Addition of Flat Dimensions:** Results in $ds^2 = ds^2_N + \sum_{i=1}^{N-2} dr_i^2$, remaining Ricci-flat.
- **Black Brane:** N-dimensional black hole horizon $S^{N-2} \times R^2 \times S^{N-2}$ times \mathbb{R}^2 .
- **Mass:** Infinite due to extra dimensions, made finite by imposing periodic boundary conditions.

Fig. D.1 Schematic illustration of the properties of conformal Killing-Yano tensors. Points inside a large oval correspond to conformal Killing-Yano tensors. Horizontal lines connect two conformal Killing-Yano tensors, related by the Hodge-duality transformation. Two triangles represent closed conformal Killing-Yano tensors and Killing-Yano tensors. The Hodge duality transformation gives a map between these objects. An exterior product maps two closed conformal Killing-Yano tensors to another closed conformal Killing-Yano tensor. A ‘square’ of a Killing-Yano tensor gives a rank-2 Killing tensor.



CKY Summary

1. **Dimensions of Spacetime:**
 - Denoted by $D=2n+\epsilon$, where $\epsilon=0$ for even dimensions and $\epsilon=1$ for odd dimensions.
 2. **Hidden Symmetry Objects:**
 - **Killing–Yano Tensor:** An antisymmetric tensor (or form).
 - **Conformal Killing–Yano Tensor:** Also an antisymmetric tensor.
 3. **Differential Forms:**
 - **Exterior (Wedge) Product:** $\alpha_p \wedge \beta_q \alpha_p \wedge \beta_q$ is a $(p+q)(p+q)$ -form.
 - **Hodge Dual:** $*\alpha_p$ is a $(D-p)(D-p)$ -form.
 - **Exterior Derivative:** $d\alpha_p$ is a $(p+1)(p+1)$ -form.

We denote the number of dimensions of the spacetime by $D = 2n + \varepsilon$, where $\varepsilon = 0$ for even dimensions, and $\varepsilon = 1$ for odd dimensions. The basic objects responsible for the hidden symmetry are, Killing–Yano tensor and conformal Killing-Yano tensor. They are antisymmetric tensors, or forms. To describe their properties it is very convenient to use the ‘language’ of differential forms (see Section 3.1.4). The exterior (or wedge) product of p -form α^p and q -form β^q is a $(p+q)$ -form $\alpha^p \wedge \beta^q$. The Hodge dual of α^p -form α^p is a $(D-p)$ -form $(\ast \alpha)^{D-p}$. An exterior derivative of the p -form α^p is a $(p+1)$ -form $d\alpha^p$. Possible iterations with a bigger pcircuit, critical space-time iterations, critical visions.

Simplified

1. The Hodge dual of a conformal Killing–Yano tensor is a conformal Killing–Yano tensor.
 2. The Hodge dual of a closed conformal Killing–Yano tensor is a Killing–Yano tensor.
 3. The Hodge dual of a Killing–Yano tensor is a closed conformal Killing–Yano tensor.
 4. An Exterior product of two closed

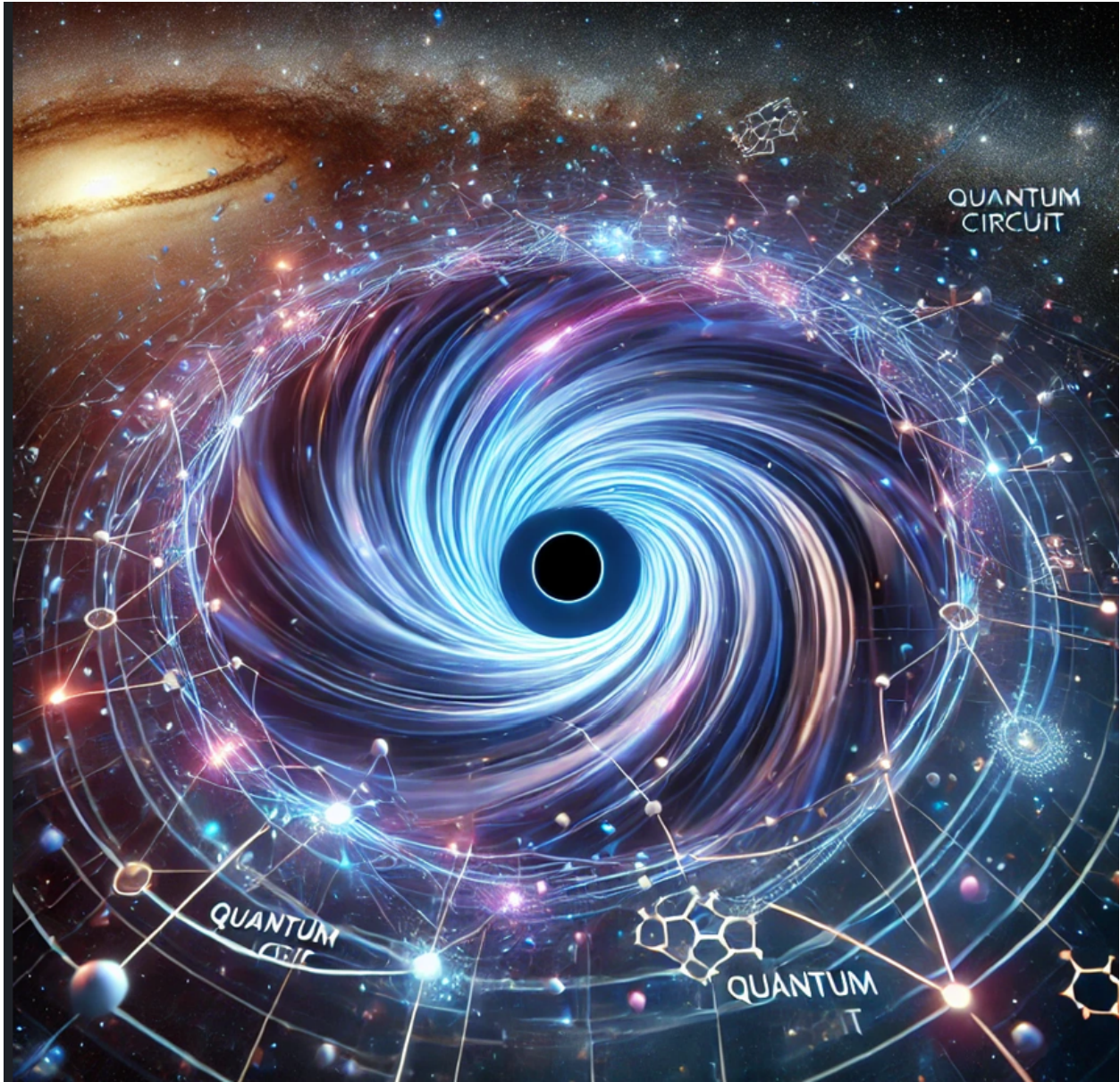
conformal Killing–Yano tensors is a closed conformal Killing–Yano tensor. Consider a 2-form h obeying the equation $h_{\mu\nu} ; \lambda = \lambda v_\mu - g \lambda \mu \xi^\nu$.

D.9.2 Killing–Yano tower Starting with a principal conformal Killing–Yano tensor h one can construct a set of new closed conformal Killing–Yano tensors $h \wedge j = h \wedge h \wedge \dots \wedge h$ j times . (D.9.3) The index j enumerates how many h s are in the exterior product, so that $h \wedge 1 = h$. For $j = n$ the object $h \wedge n$ is either proportional to the totally antisymmetric tensor (for $\varepsilon = 0$), or its dual is a vector (for $\varepsilon = 1$). Excluding these ‘trivial’ cases, one has $(n - 1)$ non-trivial closed conformal Killing–Yano tensors. The Hodge dual of these tensors $k_j = *h \wedge j$, (D.9.4) are $(n - 1)$ Killing–Yano tensors, which can be used to construct $(n - 1)$ Killing tensors $K_j = k_j \bullet k_j$.

$$B = \begin{pmatrix} \mathbf{x} & 0 & Q_A & \mathbf{e} & \mathbf{x}_0 \\ P & \bar{\mathbf{b}} \frac{\bar{\mathbf{c}}^\top Q_A}{||\bar{\mathbf{b}}||^2} & -\frac{(r+1)}{||\bar{\mathbf{b}}||^2} \bar{\mathbf{b}} & \frac{\bar{\mathbf{c}}^\top \mathbf{x}_0 - \bar{z}}{||\bar{\mathbf{b}}||^2} \bar{\mathbf{b}} & \\ \mathbf{y} & 0 & 1 & 1 & \\ \tau & 0 & 1 & 0 & \\ \theta & 0 & 1 & 0 & \\ \mathbf{s} & -A^\top P & -A^\top \bar{\mathbf{b}} \frac{\bar{\mathbf{c}}^\top Q_A}{||\bar{\mathbf{b}}||^2} & \frac{r+1}{||\bar{\mathbf{b}}||^2} A^\top \bar{\mathbf{b}} + \mathbf{e} & \frac{-\bar{\mathbf{c}}^\top \mathbf{x}_0 + \bar{z}}{||\bar{\mathbf{b}}||^2} A^\top \bar{\mathbf{b}} + \mathbf{e} \\ \kappa & \mathbf{b}^\top P & (\gamma - 1) \mathbf{c}^\top Q_A - \gamma \mathbf{e}^\top Q_A & 1 - \gamma(r+1) & -\gamma \bar{z} + (\gamma - 1) \mathbf{c}^\top \mathbf{x}_0 - \gamma \mathbf{e}^\top \mathbf{x}_0 \end{pmatrix}. \quad (C1)$$

Quantum circuits integration pack with the previous sections: Possible FPGA integration in satellites or spatial stations with quantum resources.

$$\begin{aligned} & \begin{pmatrix} 0 & A^\top & -\mathbf{c} & \bar{\mathbf{c}} \\ -A & 0 & \mathbf{b} & -\bar{\mathbf{b}} \\ \mathbf{c}^\top & -\mathbf{b}^\top & 0 & -\bar{z} \\ -\bar{\mathbf{c}}^\top & \bar{\mathbf{b}}^\top & \bar{z} & 0 \end{pmatrix} \begin{pmatrix} \Delta \mathbf{x} \\ \Delta \mathbf{y} \\ \Delta \tau \\ \Delta \theta \end{pmatrix} + \begin{pmatrix} \Delta \mathbf{s} \\ \mathbf{0} \\ 0 \end{pmatrix} \\ &= \begin{pmatrix} -A^\top \mathbf{y} + \mathbf{c} \tau - \bar{\mathbf{c}} \theta - \mathbf{s} \\ A \mathbf{x} - \mathbf{b} \tau + \bar{\mathbf{b}} \theta \\ -\mathbf{c}^\top \mathbf{x} + \mathbf{b}^\top \mathbf{y} + \bar{z} \theta \\ \bar{\mathbf{c}}^\top \mathbf{x} - \bar{\mathbf{b}}^\top \mathbf{y} - \bar{z} \tau \end{pmatrix}. \end{aligned} \quad (19)$$



Constraints n: $(w; \varphi; \rho; t; \eta) \in Q_1 \times \cdots \times Q_1^n$ n positivity constraints $\times Q_1 \times \cdots \times Q_1^m$ 2n budget constraints $\times Q_m + 1$ risk , where I denotes an identity block, 0 denotes a submatrix of all 0s, 0 is a vector of all 0s, 1 is a vector of all 1s, and the size of each block of A can be inferred from its location in the matrix. Thus, the total number of cones is $r = 3n + 1$ and the combined dimension is $N = 3n + m + 1$

$(w; \varphi; \rho; t; \eta) \in Q_1 \times \cdots \times Q_1^n$ n positivity constraints. rows of the $K \times N$ matrix A are sparse and contain only one or two nonzero entries. However, the final m rows of the matrix A will be dense and will contain $n + 1$ nonzero entries due to the appearance of the matrix M containing historical data.

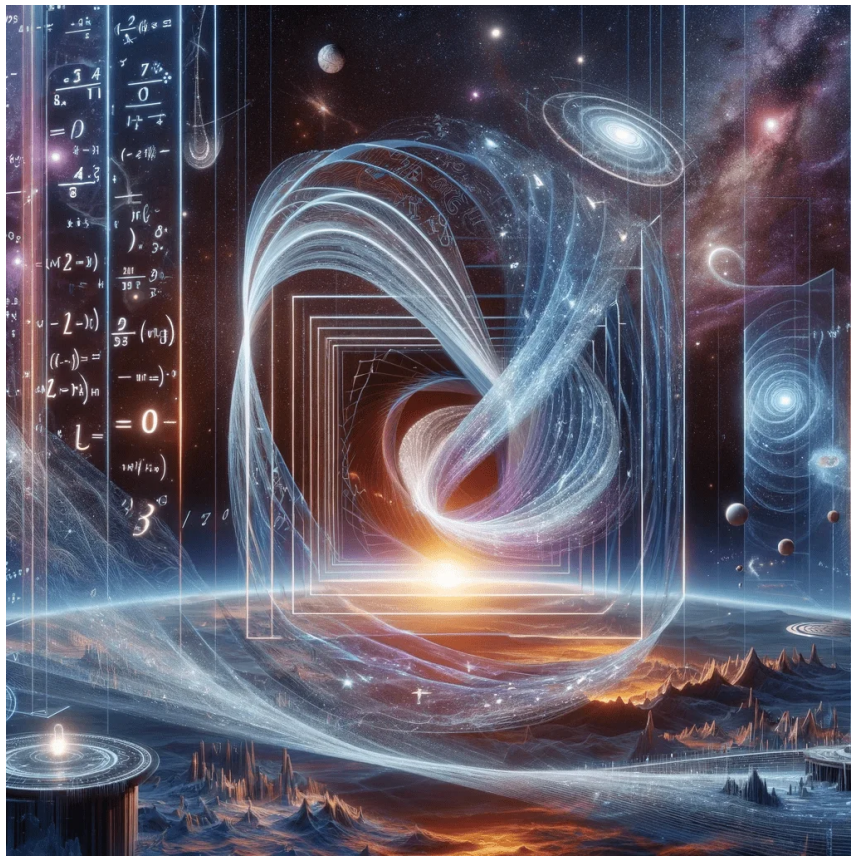
$A^\top y + s = c\tau - (c - e)\theta$, which has the trivial solution $y = 0$, $s = e$ when $\tau = 0 = 1$. Complement these with two additional linear constraints to form the program $\min_{(x; y; \tau; \theta; s; \kappa)} (r+1)\theta$ such that

$$(13) \quad | \quad 0 \ A^\top -c^\top \ c -A \ 0 \ b^\top -b \ c^\top -b^\top \ 0 \ z^\top -c^\top -b^\top -z \ 0 \quad | \quad | \quad x \ y \ \tau \ \theta \quad | + \quad | \quad s \ 0 \ \kappa \ 0 \quad | = \quad | \quad 0 \ 0 \ 0$$

r+1 |

$x, s \in Q; \tau, \kappa \geq 0; y, \theta$ free, where $b = b - Ae$, $c = c - e$, $z = c^\top e + 1$, and $r = e^\top e$ is the number of cones in the original SOCP. While Eq. (13) is not exactly of the form given Eq. (5), we may still think of it as a primal SOCP. Since the block matrix in Eq. (13) is skew symmetric and the objective-function coefficients are equal to the right-hand side of the equality constraints, when we compute the dual program [cf. Eq. (6)], we arrive at an equivalent program; we conclude that Eq. (13) is self-dual [51]. Thus, when applying path following primal-dual IPMs Eq. (13), we need only keep track of the primal variables, i.e., $x, y, \tau, \theta, s, \kappa$. Taking into account the addition of τ and κ , which are effect next repair primal-dual variables, we define the duality gap [cf. Eq. (7)] as $\mu(x, \tau, s, \kappa) := r+1 (x^\top s + \kappa \tau)$.

Black-holes-Quantum-Galactic-system;



Quantum circuits integration pack with the previous sections: Possible FPGA integration in satellites or spatial stations with quantum resources.



(Quantum integration) -

The point $(x; y; \tau; \theta; s; \kappa)$ is feasible, i.e., if it satisfies the four linear constraints Eq. (13), then we have the identity $\mu(x, \tau, s, \kappa) = -x^T A^T y + x^T c - x^T c\theta + \kappa \tau r + 1 = -b^T y^T b^T y + x^T c - x^T c\theta + \kappa \tau r + 1 = -b^T y\theta - x^T c\theta + \tau\theta r + 1 = 0$

Matrix Multiplication in the Context of a Black Hole

Given the matrix:

$$M = \begin{pmatrix} 0 & A^T & -c & c \\ -A & 0 & b & -b \\ c^T & -b^T & 0 & -z \\ -c^T & b^T & z & 0 \end{pmatrix}$$

And the vector:

$$v = \begin{pmatrix} x \\ y \\ \tau \\ \theta \end{pmatrix}$$

With the additional vector:

$$v' = \begin{pmatrix} s \\ 0 \\ \kappa \\ 0 \end{pmatrix}$$



With the additional vector:

$$v' = \begin{pmatrix} s \\ 0 \\ \kappa \\ 0 \end{pmatrix}$$

The resulting equation is:

$$Mv + v' = \begin{pmatrix} 0 \\ 0 \\ 0 \\ r+1 \end{pmatrix}$$

Expanded Form:

$$\begin{pmatrix} 0 & A^T y & -c\tau & c\theta \\ -Ax & 0 & b\tau & -b\theta \\ c^T x & -b^T y & 0 & -z\theta \\ -c^T x & b^T y & z\tau & 0 \end{pmatrix} + \begin{pmatrix} s \\ 0 \\ \kappa \\ 0 \end{pmatrix} = \begin{pmatrix} 0 \\ 0 \\ 0 \\ r+1 \end{pmatrix}$$

Scaled by Factor of 6:

$$6 \begin{pmatrix} 0 & A^T y & -c\tau & c\theta \\ -Ax & 0 & b\tau & -b\theta \\ c^T x & -b^T y & 0 & -z\theta \\ -c^T x & b^T y & z\tau & 0 \end{pmatrix} + 6 \begin{pmatrix} s \\ 0 \\ \kappa \\ 0 \end{pmatrix} = 6 \begin{pmatrix} 0 \\ 0 \\ 0 \\ r+1 \end{pmatrix}$$

Simplified Notation Example:

$$A^\top y + s = c\tau - (c - e)\theta$$